

Adduct 35: mp 223-225 °C; IR (KBr) 1753, 1702, 1460, 1250, 1120, 1050, 745 cm^{-1} ; mass spectrum, m/e (relative intensity) 227 (M^+ , 10), 184 (42), 169 (53), 156 (100). ^1H NMR and ^{13}C NMR data are summarized in Tables II and III.

Anal. ($\text{C}_{15}\text{H}_{17}\text{NO}$): C, H, N.

Diimide Reduction of 1 and 2. To a solution of 1 (182 mg, 1 mmol) in aqueous methanol (10 mL) were added 1% aqueous cupric acetate solution (0.2 mL) and 64% hydrazine (1.2 mL, 24.2 mmol). After being stirred for 20 h at room temperature under bubbling air, water (50 mL)

was added and the precipitate was collected by filtration to give 2 (184 mg, 100%) as colorless solid, mp 91-92 °C (lit.² mp 90.5-91.5 °C).

Compound 2 (92 mg, 0.5 mmol) was treated with 64% hydrazine (0.6 mL, 12.1 mmol) for 10 h under the same conditions. The workup afforded the unchanged 2 (85 mg).

Acknowledgment. We are indebted to Dr. G. L'abbé for helpful discussions in ^{13}C NMR analyses of β -lactams. We also thank Mr. E. Wakabayashi for the experimental assistance.

Catalysis of the Methoxyaminolysis of Phenyl Acetate by a Preassociation Mechanism with a Solvent Isotope Effect Maximum¹

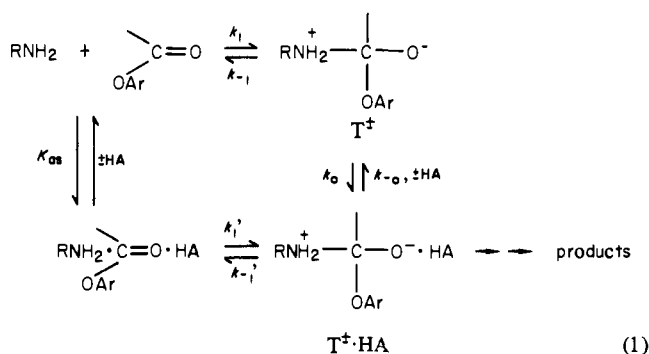
Michael M. Cox and William P. Jencks*

Contribution No. 1340 from the Graduate Department of Biochemistry, Brandeis University, Waltham, Massachusetts 02254. Received July 7, 1980

Abstract: General-acid catalysis of the reaction of methoxyamine with phenyl acetate by the proton, carboxylic acids, and ammonium ions follows a nonlinear Brønsted curve. This curve agrees quantitatively with the behavior expected for the enforced preassociation mechanism of catalysis that was predicted for this reaction. The stronger acids, including the proton, follow a Brønsted slope of $\alpha = 0.16$ that represents rate-limiting amine attack assisted by hydrogen bonding, weaker acids react with partially rate-limiting proton transfer to the addition intermediate T^\ddagger , and the weakest acids follow a steeper Brønsted slope approaching $\alpha = 1.0$ that represents rate-limiting separation of the conjugate base from the protonated intermediate T^\ddagger . There is no decrease in the rate constant for catalysis by chloroacetic acid with increasing viscosity in water-glycerol mixtures; a decrease is observed for the reaction of methylamine with *p*-tolyl acetate catalyzed by acetate buffers, which is believed to proceed by a diffusion-controlled trapping mechanism. A sharp maximum in the solvent isotope effect at $\text{p}K_{\text{HA}} = 6.8$ confirms the kinetically significant proton-transfer step in the intermediate region near $\Delta\text{p}K = 0$. The decrease with stronger acids represents a decrease in the isotope effect for this proton-transfer step, which is largely rate limiting for acids of $\text{p}K_{\text{a}} = 4-7$, but the decrease with weaker acids can be explained by the change to rate-limiting diffusional separation of T^\ddagger and A^- . Two explanations are offered for the decreased isotope effect with increasing acid strength. (1) There is a sharp change to an asymmetric structure of the transition state for the very rapid proton-transfer step, as suggested by Melander and Westheimer. (2) There is a shift to a rate-limiting change in solvation that occurs immediately either before or after the proton-transfer step with stronger acids. It is possible to fit the observed Brønsted curve and isotope effect maximum with calculated rate constants that are based on a rate law and estimated rate constants for the steps of the latter mechanism.

We describe here evidence that the reaction of methoxyamine with phenyl acetate proceeds through a tetrahedral addition intermediate, T^\ddagger , which is sufficiently unstable that the reaction is forced to proceed through a preassociation mechanism in which the amine, the ester, and a molecule of catalyzing acid come together in an encounter complex before the N-C bond is formed. We also discuss possible explanations for the sharp solvent isotope effect maximum with changing $\text{p}K_{\text{a}}$ of the catalyzing acid for this reaction, including a mechanism that involves kinetically significant solvent reorientation steps. Some of this work has been reported in preliminary communications.^{2,3}

The attack of methylamine on *p*-tolyl acetate gives an addition intermediate, T^\ddagger , that reverts to reactants with a rate constant of $k_{-1} \approx 3 \times 10^9 \text{ s}^{-1}$ if it is not trapped by protonation after encounter with a molecule of buffer acid or base (eq 1). These conclusions are based on typical "Eigen curves" for catalysis of ester formation and on a leveling of the product ratio as the acid concentration is increased when the addition intermediate is generated by addition of water to the corresponding imidate.⁴



General-acid catalysis of the aminolysis reaction involves trapping of the intermediate by encounter of T^\ddagger with a buffer acid to form the complex $T^\ddagger \cdot \text{HA}$ (k_{a} , eq 1), so that it can undergo proton transfer and go on to products rather than revert to reactants (k_{-1} or k_{-1}' , eq 1).

The complex $T^\ddagger \cdot \text{HA}$ may also be formed through an alternative route by a preassociation mechanism. In this mechanism the reactants and catalyst come together in an encounter complex prior to addition of the amine, as shown in the lower path through K_{as}

(1) Supported by grants from the National Science Foundation (Grant BG-31740) and the National Institutes of Health (Grants GM20888 and GM20168). M.M.C. was supported by a training grant from the National Institutes of Health (Grant 5-T01-GM00212).

(2) Cox, M. M.; Jencks, W. P. *J. Am. Chem. Soc.* **1978**, *100*, 5956-5957.

(3) Cox, M. M.; Jencks, W. P. *Fed. Proc., Fed. Am. Soc. Exp. Biol.* **1979**, *38*, 473.

(4) Satterthwait, A. C.; Jencks, W. P. *J. Am. Chem. Soc.* **1974**, *96*, 7031-7044.

and k_1' in eq 1. Although termolecular collisions are rare in the gas phase, formation of an encounter complex containing three molecules in solution is not improbable and requires no more loss of entropy than the formation of $T^{\ddagger}\cdot HA$ through the upper path of eq 1.⁵ As the addition intermediate T^{\ddagger} is made progressively less stable, a point will be reached at which it will break down to reactants within the encounter complex $T^{\ddagger}\cdot HA$ (k_{-1}') faster than the acid diffuses away from this complex (k_{-a}). The lowest energy route for the breakdown of this complex to reactants is then through the lower, preassociation pathway, and the same pathway must be the lowest energy route for the formation of $T^{\ddagger}\cdot HA$. This point is illustrated by Gibbs' free-energy diagrams for the formation and cleavage of the intermediate $T^{\ddagger}\cdot HA$.⁶ If the catalyzing acid is forced to be present next to the carbonyl group during the addition step of the preassociation mechanism (k_1'), it is likely that it will stabilize the transition state by hydrogen bonding to the developing negative charge on the carbonyl oxygen atom. Evidence for preassociation mechanisms in general-acid-base-catalyzed reactions has been reported for carbinolamine formation from substituted benzaldehydes,^{7,8} the addition of thiol anions to acetaldehyde,⁹ the reaction of 4-methoxyphenyl formate with semicarbazide,¹⁰ the addition of weakly basic amines to formaldehyde,¹¹ and the oxidation of methionine by iodine.¹²

It was therefore predicted that the mechanism of catalysis for the aminolysis of phenyl acetate would change from a trapping mechanism for the reaction with methylamine ($k_{-1} \approx 3 \times 10^9 \text{ s}^{-1}$) to a preassociation mechanism as the attacking amine is made less basic and T^{\ddagger} becomes less stable (k_{-1} and k_{-1}' increase).⁶ The experiments reported here were carried out to test this prediction. We chose to examine methoxyamine, which is 6 pK units less basic than methylamine but reacts rapidly enough to make kinetic measurements feasible.

Experimental Section

Materials. Inorganic salts, reagent grade methanol, fluoroacetone hydrates (Aldrich, Wateree Chemical), and acetic acid were used without further purification. Other organic reagents, including tetramethylammonium chloride, were purified by distillation or recrystallization before use. Phenyl acetate was purified by a published procedure¹³ and a similar procedure was used for *p*-tolyl acetate. Methoxyamine hydrochloride (Eastman) was recrystallized three times from ethanol-ether, and disodium methylarsenate was prepared as described previously.¹⁴ Aminoacetonitrile hydrochloride required repeated treatments with decolorizing carbon and recrystallization from aqueous ethanol. Pentafluoroacetone hydrate solutions were prepared by bubbling pentafluoroacetone gas into cold water and were standardized by weight and titration. Glycerol was distilled under vacuum, after adding sodium and heating of the solution for 3 h at 80 °C.

S-Methyl-L-cysteine methyl ester hydrochloride was prepared¹⁵ by the dropwise addition of 50 mL of thionyl chloride to 25 g of *S*-methyl-L-cysteine (Sigma) in 600 mL of refluxing methanol. After 30 min 26 g of formic acid was added, the solvent was removed, and the white solid was recrystallized from methanol-ether (81%) and 2-propanol; mp 143–144 °C (lit.¹⁶ 142–143 °C).

Kinetic Measurements. Pseudo-first-order rate constants were usually determined spectrophotometrically by measuring the initial rate (<3% reaction) of phenol release at 275 nm (277 nm for *p*-tolyl acetate) at 25 °C and ionic strength 1.0 M, maintained with potassium chloride. Solutions of methoxyamine hydrochloride were neutralized shortly before

use, mixed with buffer solutions, and incubated for 5–10 min at 25 °C. Reactions were initiated by the addition of 1.0 mL of 0.03 M phenyl acetate to give a volume of 3.0 mL. First-order rate constants were obtained by dividing the initial rate of change of absorbance by the final absorbance, A_{∞} , which was determined after alkaline hydrolysis and neutralization of an aliquot of the phenyl acetate solution that was used for each experiment. The initial absorbance showed <2% phenol in the reaction mixtures. Between pH 8.5 and 9.2 a correction was made for absorbance due to phenolate ion based on a pK for phenol¹³ of 9.86 and $\epsilon_{\text{PhO}^-} = 1.3\epsilon_{\text{PhOH}}$ at 275 nm. Above pH 9.2 pseudo-first-order rate constants were measured directly after the addition of 0.06–0.1 mL of 0.03 M phenyl acetate to reaction mixtures containing a large excess of amine. First-order plots were linear to ≥ 3 half-times, and satisfactory agreement was found between initial rate and pseudo-first-order rate constant measurements with triethylenediamine buffers at pH 9.22.

The pH showed negligible change during experiments and usually varied by <0.1 unit with increasing buffer concentration. Corrections were not made for these pH changes because it was found that the apparent pK of methoxyamine hydrochloride showed similar changes under the same or similar conditions.¹⁷ Most buffers that might react with methoxyamine such as chloroacetate and amino acid esters showed no significant change in pH on incubation with methoxyamine and were shown to give the same rate constants for the reaction with phenyl acetate after a preliminary incubation corresponding to the time of a kinetic run. However, methoxyamine adds to fluoroacetone hydrates, and equilibrium constants for the addition reaction of 3.3 M⁻¹ for pentafluoroacetone hydrate and 0.7 M⁻¹ for hexafluoroacetone hydrate were determined from the observed decrease in pH upon mixing buffers containing methoxyamine and the hydrate. Correction for the decrease in methoxyamine free-base concentration gave a 40–60% increase in the observed catalytic constants for these compounds, so that the corrected constants are approximate values.

The experimental conditions for determination of catalytic constants for the reactions with methoxyamine are given in Table SI in the supplementary material.

The effect of viscosity on rate constants was determined in aqueous glycerol, prepared by mixing 90% (v/v) glycerol with buffer solutions. Viscosities were determined at 25 °C with Cannon-Fenske viscosimeters relative to 1.0 and 2.0 M potassium chloride.

Solvent deuterium isotope effects were determined from measurements in protium and deuterium oxide solutions by using identical buffer compositions. Parallel experiments in the two solvents were usually carried out on the same day. The isotopic composition of the deuterium oxide solutions was always >97% deuterium after addition of all reagents. The pD of deuterium oxide solutions was obtained by adding 0.4 to the observed pH meter reading.¹⁸

Calculated Brønsted Curves. Theoretical Brønsted curves for diffusion-controlled trapping and preassociation mechanisms were calculated as described previously^{7,9} by using the rate and equilibrium constants that are given in the text. The "Eigen curve" for the trapping mechanism was calculated from eq 2, and the curve for a preassociation mechanism was

$$k_A = \frac{K_1 k_a k_p k_b}{k_p k_b + k_{-a} k_b + k_{-a} k_{-p}} \quad (2)$$

calculated from eq 3, in which the rate constants are defined in eq 1 and 6, $K_1 = k_1/k_{-1}$, and $k_{\text{HA}}^{\text{dc}}$ is the rate constant for a trapping mechanism

$$k_A = \frac{k_{\text{HA}}^{\text{dc}} [k_{-a} + k_{-1} \text{antilog} [\alpha(15.74 - \text{p}K_{\text{HA}})]] (k_p k_b / k_{-a})}{k_p k_b + [k_{-a} + k_{-1} \text{antilog} [\alpha(15.74 - \text{p}K_{\text{HA}})]] (k_b + k_{-p})} \quad (3)$$

when encounter of HA and T^{\ddagger} is rate limiting. Rate constants for diffusion-controlled steps were chosen to fit the curves reported by Eigen.¹⁹ Equation 3 gives the observed rate constant in terms of contributions of the rate constant that would be observed for a trapping mechanism and the rate increase that is brought about in a preassociation mechanism as a consequence of the rapid breakdown of T^{\ddagger} (k_{-1}) and stabilization of the transition state by hydrogen bonding ($\alpha[15.74 - \text{p}K_{\text{HA}}]$).²⁰ We have chosen to neglect hydrogen bonding in the complex $T^{\ddagger}\cdot HA$ because we have no way of estimating the strength of this hydrogen bond. This has no effect on the calculated overall rate constants, energies of the transition states, or rate constant ratios k_{-1}'/k_{-a} and k_{-1}'/k_p . Such hydrogen bonding certainly exists and will have the effect of lowering the energy of the well for $T^{\ddagger}\cdot HA$ and decreasing the absolute values of the rate constants k_{-1}' and k_p below the values of k_{-1} and k_p used

(5) If the equilibrium constants for the formation of the encounter complexes A·B from A and B and A·B·C from A·B and C are 0.1 M⁻¹, the equilibrium constant for the formation of A·B·C from A, B, and C is 0.01 M⁻². The termolecular complex is undoubtedly formed in two consecutive steps not through a termolecular collision.

(6) Jencks, W. P. *Acc. Chem. Res.* **1976**, *9*, 425–432.

(7) Sayer, J. M.; Jencks, W. P. *J. Am. Chem. Soc.* **1973**, *95*, 5637–5649.

(8) Sayer, J. M.; Edman, C. *J. Am. Chem. Soc.* **1979**, *101*, 3010–3016.

(9) Gilbert, H. F.; Jencks, W. P. *J. Am. Chem. Soc.* **1977**, *99*, 7931–7947.

(10) Ortiz, J. J.; Cordes, E. H. *J. Am. Chem. Soc.* **1978**, *100*, 7080–7082.

(11) Abrams, W. R.; Kallen, R. G. *J. Am. Chem. Soc.* **1976**, *98*, 7777–7789.

(12) Young, P. R.; Hsieh, L.-S. *J. Am. Chem. Soc.* **1978**, *100*, 7121–7122.

(13) Jencks, W. P.; Gilchrist, M. *J. Am. Chem. Soc.* **1968**, *90*, 2622–2637.

(14) Fox, J. P.; Jencks, W. P. *J. Am. Chem. Soc.* **1974**, *96*, 1436–1449.

(15) Boissonnas, R. A.; Guttman, St.; Jaquenoud, P.-A.; Waller, J.-P. *Helv. Chim. Acta* **1956**, *39*, 1421–1427.

(16) Damoglou, A. P.; Lindley, H.; Stapleton, I. W. *Biochem. J.* **1971**, *123*, 379–384.

(17) Hogg, J. L.; Jencks, W. P. *J. Am. Chem. Soc.* **1977**, *99*, 4772–4778.

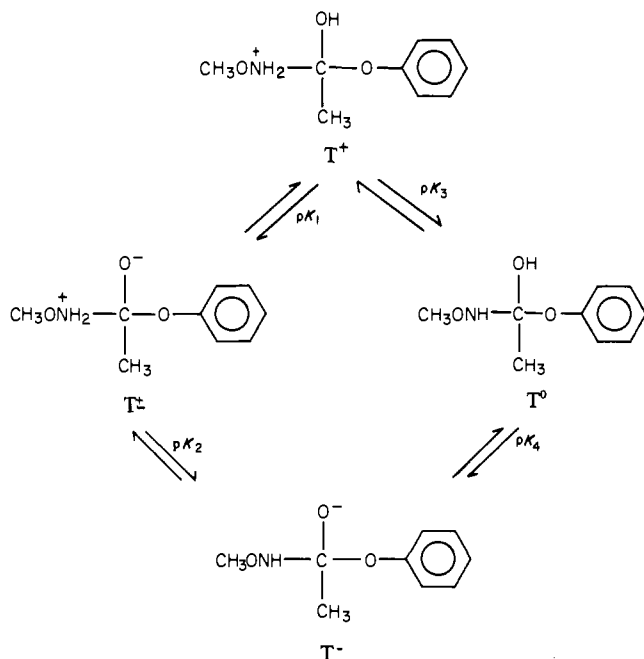
(18) Pentz, L.; Thornton, E. R. *J. Am. Chem. Soc.* **1967**, *89*, 6931–6938.

Glascow, P. K.; Long, F. A. *J. Phys. Chem.* **1960**, *64*, 188–190.

(19) Eigen, M. *Angew. Chem., Int. Ed. Engl.* **1964**, *3*, 1–19.

(20) Jencks, W. P.; Gilbert, H. F. *Pure Appl. Chem.* **1977**, *49*, 1021–1027.

Scheme I



here.²⁰ Sayer and Edman⁸ have chosen to assume a value of $\alpha = 0.11$ for stabilization of T^{\pm} -HA by hydrogen bonding so that the absolute values of some microscopic rate constants are different for calculations based on their procedure and on eq 3, but there is no difference in the overall rate constants or Brønsted curves calculated by the two procedures.

Estimation of pK values. The equilibrium constants for protonic equilibria of the tetrahedral addition intermediates (Scheme I) were estimated as described previously by using a value of $\rho_1 = 8.4$ for the dissociation constants of substituted ammonium ions and alcohols.^{7,14,21}

The value of pK_1 was estimated to be 6.4, on the basis of $pK = 9.98$ for the hydroxyl group of $CH_3NH_2CH_2OH^+$,²² $\sigma_1 = 0.38$ for OPh,²³ and corrections of +0.3 for CH_3 and -0.7 for the substitution of CH_3ONH_2 for CH_3NH_2 .¹⁴

The value of pK_3 was estimated to be 0, on the basis of $pK = 4.75$ for $CH_3NH_2OCH_3^+$ and corrections of +0.3 for CH_3 , -1.88 for OH, and -3.19 for OPh.¹⁴

The value of pK_4 was estimated to be 11.2, on the basis of $pK = 15.9$ for CH_3CH_2OH ,²⁴ $\sigma_1 = 0.18$ for $NHOCH_3$,¹⁴ and a correction of -3.19 for OPh. The value of pK_2 is then 4.8 from the relationship $pK_2 = pK_4 - pK_1 + pK_3$. These pK_a values are estimated to be correct to within ± 1.5 units.

Results

The disappearance of phenyl acetate in the presence of methoxyamine and buffers was found to follow the rate law of eq 4.

$$k_{\text{obsd}} = k_0 + k_w[\text{MeONH}_2] + k_A[\text{MeONH}_2][\text{HA}] + k_B[\text{MeONH}_2][\text{B}] \quad (4)$$

The rate constant for the methoxyamine-independent cleavage of phenyl acetate, k_0 , is given by eq 5. Values of k_{buf} were

$$k_0 = k_{\text{HOH}}[\text{HOH}] + k_{\text{H}}[\text{H}^+] + k_{\text{OH}}[\text{OH}^-] + k_{\text{buf}}[\text{buffer}] \quad (5)$$

determined in each experiment from the slopes of plots of k_{obsd} against buffer concentration in the absence of methoxyamine. The intercepts of these plots gave values of $k_{\text{HOH}} = 3 \times 10^{-10} \text{ M}^{-1} \text{ s}^{-1}$, $k_{\text{H}} = 8.2 \times 10^{-5} \text{ M}^{-1} \text{ s}^{-1}$, and $k_{\text{OH}} = 1.75 \text{ M}^{-1} \text{ s}^{-1}$, in which k_{H} and k_{OH} are based on $10^{-\text{pH}}$ and $10^{\text{pH}-14}$, respectively. These values agree with previously reported values of k_{HOH} ¹³ and k_{OH} ,²⁵ taking account of the empirical relationship $[\text{OH}^-] = (1.3 \pm 0.1) \times$

Table I. Rate Constants for General-Acid Catalysis of the Methoxyaminolysis of Phenyl Acetate^a

catalyst	pK_a	$k_A, \text{M}^{-2} \text{s}^{-1}$
H_3O^+	-1.74	$7.1 \times 10^{-2} \text{ }^b$
H_2O^c	15.74	$(3.4 \pm 1.5) \times 10^{-8} \text{ }^c$
dichloroacetic acid	1.03 ^d	8.3×10^{-3}
cynoacetic acid	2.23 ^e	6.3×10^{-3}
chloroacetic acid	2.65 ^e	5.8×10^{-3}
methoxyacetic acid	3.33 ^e	5.2×10^{-3}
D_2O		3.58×10^{-3}
glycolic acid	3.62 ^f	4.0×10^{-3}
D_2O		2.78×10^{-3}
acetic acid	4.6 ^e	3.25×10^{-3}
1,2,4-triazole	2.58 ^e	1.4×10^{-2}
pyrazole	2.74 ^d	1.37×10^{-2}
methoxyamine	4.72 ^e	1.45×10^{-3}
D_2O		8.3×10^{-4}
aminoacetonitrile	5.55 ^d	3.3×10^{-4}
D_2O		1.2×10^{-4}
trifluoroethylamine	5.81 ^g	1.7×10^{-4}
D_2O		4.7×10^{-5}
aspartic acid dimethyl ester	6.71 ^d	3.52×10^{-5}
D_2O		9.17×10^{-6}
S-methyl-L-cysteine methyl ester	6.92 ^d	2.98×10^{-5}
D_2O		8.3×10^{-6}
1,2-diamino-2-methylpropane ^h	6.93 ⁱ	3.62×10^{-5}
D_2O		1.22×10^{-5}
serine methyl ester	7.28 ^d	1.67×10^{-5}
D_2O		7.3×10^{-6}
ethylenediamine	7.5 ^d	3.03×10^{-5}
D_2O		1.47×10^{-5}
glycine ethyl ester	7.9 ^e	1.6×10^{-5}
aminopropionitrile	8.03 ^d	1.08×10^{-5}
D_2O		5.5×10^{-6}
chloroethylamine	8.81 ^d	$< 6.7 \times 10^{-6} \text{ }^j$
ethylamine	10.97 ^k	$< 1.25 \times 10^{-6} \text{ }^j$
triethylenediamine (DABCO)	3.47 ^h	6.5×10^{-3}
hexafluoroacetone hydrate	6.45 ^l	$\leq 2.5 \times 10^{-4} \text{ }^j$
pentafluoroacetone hydrate	7.67 ^l	$\leq 3.17 \times 10^{-5} \text{ }^j$
hexafluoro-2-propanol	9.3 ^e	$< 6 \times 10^{-6} \text{ }^j$
D,L-O-methylserine	9.18 ^d	6.2×10^{-6}

^a 25 °C, ionic strength maintained at 1.0 M with potassium chloride. ^b Based on concentration. ^c From $k_w/55.5 \text{ M}$, based on the average of three experiments. ^d This work. ^e Reference 14. ^f Young, P. R.; Jencks, W. P. *J. Am. Chem. Soc.* 1977, 99, 1206. ^g St. Pierre, T.; Jencks, W. P. *Ibid.* 1968, 90, 3817. ^h A statistical correction of $p = 6$ was used for this compound, although the two amino groups are not equivalent. However, since the pK 's of *tert*-butylamine (10.55) and methylamine (10.62) differ by only 0.07 pK unit, the difference in pK of the amino groups in 1,2-diamino-2-methylpropane is expected to be insignificant. ⁱ Page, M. I.; Jencks, W. P. *J. Am. Chem. Soc.* 1972, 94, 8818. ^j Upper limit. ^k Reference 13. ^l Reference 4.

$10^{\text{pH}-14}$ at ionic strength 1.0 M.²⁶

Apparent second-order rate constants for the reaction with methoxyamine, k^* , were obtained from $k^* = (k_{\text{obsd}} - k_0)/[\text{MeONH}_2]$ and were plotted against buffer concentration, as illustrated for the reaction with acetate buffers in Figure 1. The slopes of these plots, k_{cat} , were separated into the rate constants for catalysis by the acidic and basic components of the buffer, k_A and k_B , by using plots against the fraction of base in each buffer as illustrated in Figure 2 for the reaction in methoxyamine buffers. The values of k_A are given in Table I. Values of k_{cat} are given in Table SI in the supplementary material. For buffers that showed no significant catalysis an upper limit to the catalytic constant was estimated by assuming that a 10% rate increase was caused by catalysis at the highest buffer concentration examined but was not detected. Rate constants for the "water" and proton-catalyzed reactions were obtained from the intercepts of plots of $(k_{\text{obsd}} - k_0)/[\text{MeONH}_2]$ against the concentration of methoxyamine buffers. The former value is only approximate because of the small intercepts at $\text{pH} > 5.0$. Catalysis by hydroxide ion

- (21) Page, M. I.; Jencks, W. P. *J. Am. Chem. Soc.* 1972, 94, 8828-38.
 (22) Hine, J.; Craig, J. C., Jr.; Underwood, J. G., II; Via, F. A. *J. Am. Chem. Soc.* 1970, 92, 5194-5199.
 (23) Charton, M. J. *Org. Chem.* 1964, 29, 1222-1227.
 (24) Takahashi, S.; Cohen, L. A.; Miller, H. K.; Peake, E. G. *J. Org. Chem.* 1971, 36, 1205-1209. Hine, J.; Koser, G. F. *Ibid.* 1971, 36, 1348-1351.
 (25) Kirsch, J. F.; Jencks, W. P. *J. Am. Chem. Soc.* 1964, 86, 837-846.

- (26) Gilbert, H. F.; Jencks, W. P. *J. Am. Chem. Soc.* 1979, 101, 5774-5779.

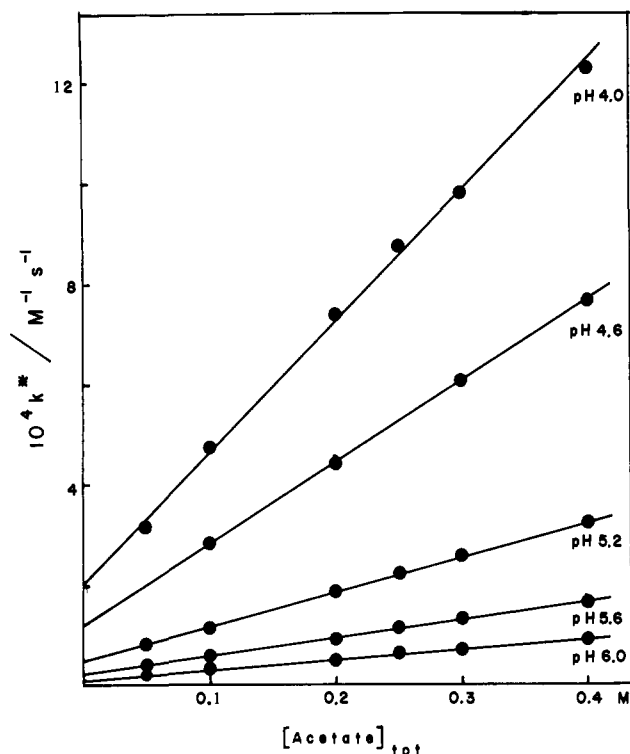


Figure 1. Catalysis of the methoxyaminolysis of phenyl acetate by acetate buffers at 25 °C and ionic strength 1.0 M (KCl).

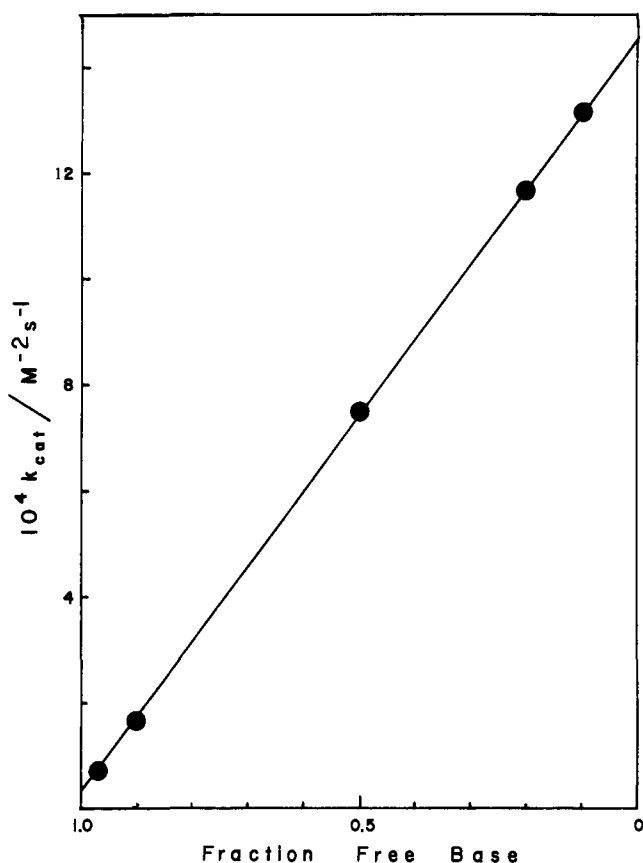


Figure 2. The dependence of observed catalytic constants for the methoxyaminolysis of phenyl acetate on the fraction free base of the methoxyamine buffer. The intercepts on the right and left ordinates are k_A and k_B , respectively.

was not significant under the conditions of the experiments.

Plots of k^* against buffer concentration were found to be linear except for chloroacetate, cyanoacetate, triazole, and pyrazole

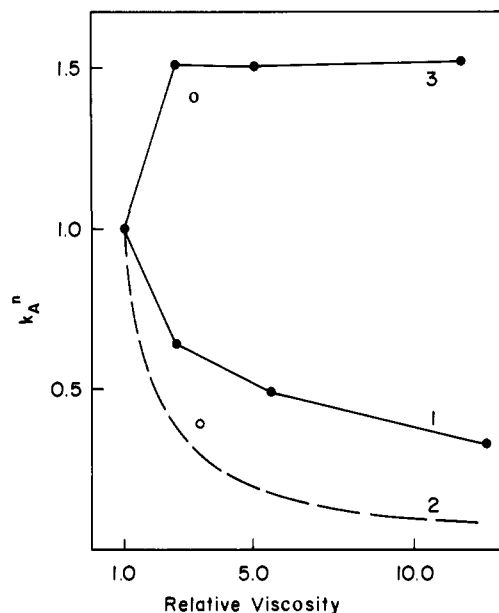


Figure 3. The effect of increasing viscosity in glycerol-water (●) and ethylene glycol-water (○) mixtures at 25 °C on the methoxyaminolysis of phenyl acetate catalyzed by chloroacetic acid (upper curve, pH 2.65, ionic strength 1.0 M, KCl) and the methylaminolysis of *p*-tolyl acetate catalyzed by acetate buffers (lower solid curve, pH 5.2, ionic strength 2.0 M, KCl). The lower dashed line was calculated for a simple inverse dependence of rate constants on viscosity. The rate constants have been normalized to 1.0 in water.

buffers. For chloroacetate buffers the curvature increased with increasing acid concentration and gave a 45% decrease from linearity at 2 M buffer, pH 2.0, but little or no nonlinearity at high pH values. The nonlinearity could be accounted for empirically by an association constant of 0.25 M⁻¹ for the formation of an inactive dimer of chloroacetic acid but may actually represent association of the acid with phenyl acetate or a solvent effect. The addition of 2 M acetamide to chloroacetate buffers was found to decrease k_{cat} by 16%. The values of k_{cat} were obtained from the initial slopes of k^* against buffer concentration, which were found to agree with values obtained from double reciprocal plots of the data. The curvature with pyrazole and triazole buffers is also most significant at low pH values and probably represents an interaction of the cationic acidic species of the buffer with phenyl acetate, since it is unlikely that the cation would dimerize.

Statistical corrections²⁷ were applied to rate and dissociation constants in Brønsted plots. A statistical correction of $p = 1.7$ for the conjugate acid of triazole was based on the difference of 1 unit in the pK of the 1,4- and 1,2-protonated species²⁸ and the Brønsted slope of $\alpha = 0.16$ for acids in this pK region.

Specific salt and solvent effects are small under the conditions used to determine the catalytic rate constants. There is no effect of substituting 0.8 M ethylammonium chloride for 0.8 M potassium chloride at pH 4.2 or of using tetramethylammonium chloride instead of potassium chloride to maintain constant ionic strength for catalysis by glycine ethyl ester at pH 5.0. Increasing the ionic strength from 1.0 to 1.2 M gives <3% rate increase in the presence of 0.05 M methoxyamine and 0.2 M ethylphosphonate buffer at pH 8.2. Addition of 1.2 M acetonitrile gives a 10% decrease and 1.2 M ethanol or methanol gives a 1–3% increase in the observed rate constant at pH 3.0 with 0.4 M methoxyamine hydrochloride and 0.8 M cyanoacetate buffer; 0.25 M isopropyl alcohol has no effect on the observed rate constant with 0.04 M methoxyamine buffer at pH 5.3.

Catalysis of the methoxyaminolysis of phenyl acetate by chloroacetic acid is increased by approximately 50% in the presence of 30–60% glycerol or 45% ethylene glycol, as shown by the open

(27) Bell, R. P.; Evans, P. G. *Proc. R. Soc. London, Ser. A* 1966, 291, 297–323.

(28) Reference 14, footnote 16.

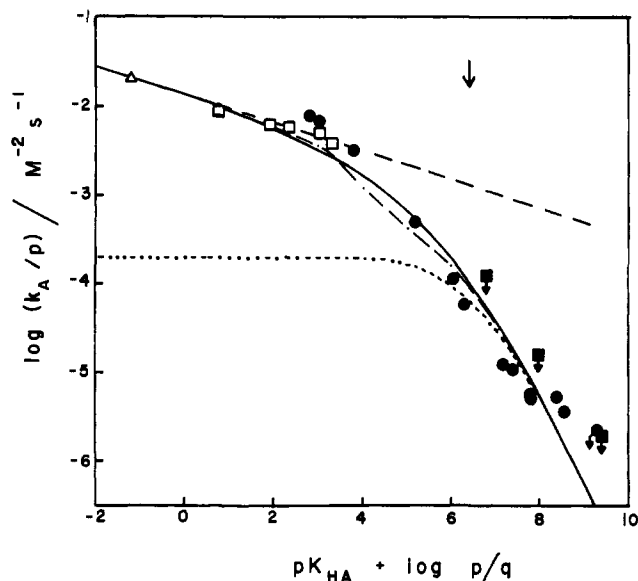


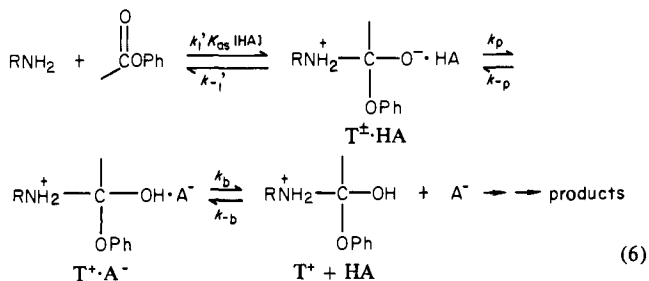
Figure 4. Brønsted plot for general-acid catalysis of the reaction of methoxyamine with phenyl acetate (25 °C, ionic strength 1.0 M, KCl) by carboxylic acids (\square), protonated amines (\bullet), fluoroacetone hydrates and hexafluoro-2-propanol (\blacksquare), and the solvated proton (Δ). The solid line is calculated for a preassociation mechanism with hydrogen bonding by using eq 3. The dotted line is calculated for a trapping mechanism by using eq 2, and the dot-dash line is calculated including kinetically significant solvation changes by using eq 3 and 8; the rate constants are given in the text and Table II. The dashed line is drawn for hydrogen bonding with $\alpha = 0.16$. The arrow at $pK = 6.4$ shows the calculated pK of T^+ . The rate constants with arrows represent upper limits.

and closed circles, respectively, in the upper curve of Figure 3; however, 45% methanol was found to cause a 32% decrease in the rate of this reaction. In contrast, catalysis of the methylaminolysis of *p*-tolyl acetate by acetate buffers is decreased in the presence of glycerol and ethylene glycol, as shown in the lower curve of Figure 3; 30% methanol was found to cause the same decrease as 45% ethylene glycol.

Figures illustrating catalysis by *S*-methyl-L-cysteine methyl ester in water and deuterium oxide and the effects of methoxyamine and chloroacetate buffers on the observed rate constants are included in the supplementary material.

Discussion

The Brønsted plot for general-acid catalysis of the reaction of methoxyamine with phenyl acetate by carboxylic acids, protonated amines, fluoroacetone hydrates, and hexafluoro-2-propanol is shown in Figure 4. Evidence for a similar Brønsted curve for the reaction of methoxyamine with *p*-nitrophenyl acetate has been reported by Cordes and co-workers.²⁹ This Brønsted plot provides evidence for the predicted preassociation mechanism for general-acid catalysis (eq 1).² In this mechanism three different, sequential steps become largely or entirely rate limiting, so that the Brønsted line curves downward as the pK of the catalyzing acid increases. These steps are shown in eq 6.



(29) Do Amaral, L.; Koehler, K.; Bartenbach, D.; Pletcher, T.; Cordes, E. H. *J. Am. Chem. Soc.* **1967**, *89*, 3537–3545.

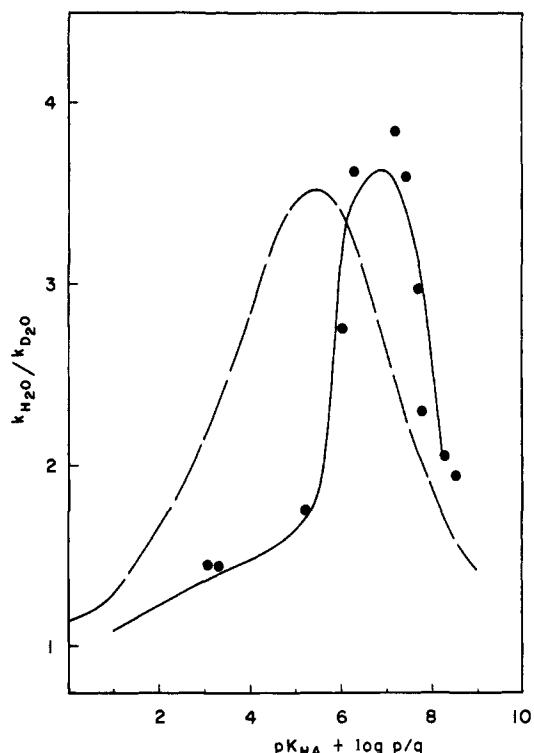
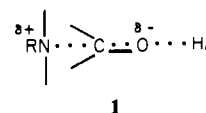


Figure 5. Solvent deuterium isotope effects for catalysis of the reaction of methoxyamine with phenyl acetate by monofunctional general acids and carboxylic acids. The dashed line was calculated by assuming a constant isotope effect on the proton transfer step (k_p , eq 6), and the solid line was calculated by assuming kinetically significant solvation changes according to eq 7, as described in the text and Table II.

(1) The rate-limiting step with the stronger acids is attack of methoxyamine on the ester with the catalyzing acid present in a position in which it can rapidly protonate the oxygen atom of the addition intermediate ($k_A = k_1'K_{as}$, eq 1 and 6). The rate constants for these acids follow a Brønsted slope of $\alpha = 0.16$ (dashed line, Figure 4), which means that the acids provide a modest stabilization of the transition state by hydrogen bonding to the developing negative charge on the oxygen atom. Such hydrogen bonding favors a preassociation mechanism relative to the diffusion-controlled step of a trapping mechanism.⁹ The rate constant for catalysis by the solvated proton fits on this Brønsted line and does not show the large positive deviation that is expected for a diffusion-controlled trapping mechanism.¹⁹ There is no significant difference between the catalytic constants for carboxylic acids and for protonated amines of comparable pK_a , shown by the open squares and closed circles, respectively, in Figure 4, so that there is no advantage of either of these classes of acids over the other for catalysis of the addition step by hydrogen bonding. The solvent deuterium isotope effects for catalysis by carboxylic acids are $k_{\text{HA}}/k_{\text{DA}} = 1.4 - 1.5$ (Table I), which is also reasonable for hydrogen bonding. The transition state for this step may be described by **1**.



(2) As the acid becomes weaker, the proton-transfer step becomes largely rate limiting (k_p , eq 6) and the Brønsted curve bends downward with an increase in α (Figure 4). This step is responsible for the appearance of a solvent isotope effect with a sharp maximum value of $k_{\text{HA}}/k_{\text{DA}} = 4$ for acids of pK_a near 7 (Figure 5). The downward curvature in the Brønsted plot begins at pK_a values well below the estimated pK_a of 6.4 for the addition intermediate, as expected for a preassociation mechanism;⁷ lines of slope 0 and 1.0 drawn through the points for the strong and

weak acid catalysts intersect at $pK_a = 4.8$.

The nonlinear Brønsted curve cannot be accounted for by two separate linear correlations with different slopes for catalysis by oxygen acids and by protonated amines, because the catalytic constants for fluoroacetone hydrates and hexafluoro-2-propanol (closed squares, Figure 4) fall far below the line of $\alpha = 0.16$ that is followed by carboxylic acids and the solvated proton. Furthermore, there is no reason to believe that protonated amines should be much better catalysts than oxygen acids, as would be required if a straight line drawn through the catalytic constants for protonated amines were extended to catalysts of lower pK_a .

(3) As the acid becomes still weaker, diffusion away of the conjugate base of the catalyst from the protonated addition intermediate becomes rate limiting (k_b , eq 6), the Brønsted slope bends further downward to approach a slope of $\alpha = 1.0$ (Figure 4), and the solvent isotope effect decreases sharply. In the reverse direction this step would correspond to diffusion-controlled encounter of A^- with T^+ , followed by rapid proton transfer and breakdown of T^\ddagger .

Steps 2 and 3 are the same as those for a trapping mechanism according to the classical Eigen scheme for proton transfer between electronegative atoms.¹⁹ The preassociation mechanism differs from the trapping mechanism in that there is a faster, lower energy pathway for formation of the critical intermediate $T^\ddagger \cdot HA$ by preassociation of the reactants (K_{aa} and k_1' , eq 1) that avoids the diffusion-controlled encounter of T^\ddagger with HA in the trapping mechanism (k_a , eq 1). This is shown in Figure 4, in which the dotted line represents an "Eigen curve" for catalysis by the trapping mechanism, and the solid line is calculated for the preassociation mechanism. The two curves merge for weak acid catalysts, but the trapping mechanism gives a leveling off with smaller rate constants for acids of $pK_a < 6$ compared with the preassociation mechanism.

The theoretical curves were calculated from eq 2 and 3 and from values of $pK_{T^+} = 6.5$, $k_{-1} = 2 \times 10^{10} \text{ s}^{-1}$, $k_b = k_{-a} = 10^{11} \text{ s}^{-1}$, $\log k_p = 11 + 0.5\Delta pK$, $\log k_{-p} = 11 - 0.5\Delta pK$, $k_{HA}^{dc} = 2 \times 10^{-4} \text{ M}^{-2} \text{ s}^{-1}$, and $\alpha = 0.16$. The values for k_p and k_{-p} of 10^{11} s^{-1} at $\Delta pK = 0$ give a somewhat better fit to the data than the values of 10^{10} s^{-1} that were used previously for similar calculations,^{7,9,30} but reasonable agreement with the data can be obtained with some variation in the absolute values of most of the rate constants. For example, a satisfactory fit may be obtained if k_{-1} is increased by 50% and k_{HA}^{dc} is decreased by the same amount or if k_p and k_{-p} are both decreased by a factor of 3. Values for k_b and k_{-a} were chosen to fit the curves reported by Eigen,¹⁹ and the value of k_{HA}^{dc} corresponds to the horizontal portion of the dotted line in Figure 4. The energy of the transition state for the k_{-1}' step is lower than that for the k_{-1} step (in both directions) because of stabilization by hydrogen bonding, as described above; these steps correspond to the rate constants k_A and k_{HA}^{dc} , respectively, in the forward direction for acids of $pK_a < 4$. The barrier for the proton-transfer step, k_p , may become vanishingly small for strong acids, in the region in which the k_1' step is rate determining.

The observed rate constants for a diffusion-controlled trapping mechanism should decrease with increasing viscosity of the solvent, whereas no such decrease should be observed for a preassociation mechanism that avoids the diffusion step. The methylaminolysis of *p*-tolyl acetate catalyzed by acetate buffers is inhibited and the rate of methoxyaminolysis of phenyl acetate catalyzed by chloroacetic acid increases with increasing viscosity in glycerol-water and ethylene glycol-water mixtures, consistent with this expectation (Figure 3), although the decrease in the rate of the former reaction is smaller than predicted for an inverse dependence of the rate constant on viscosity (dashed line, Figure 3). These

observations support the preassociation mechanism for the methoxyaminolysis reaction but do not provide rigorous proof of the mechanism because of an unexplained inhibitory effect of methanol on the two reactions. This means that methanol is not a satisfactory model for the solvent effect of glycerol so that it is not possible to evaluate the extent to which the data in Figure 3 include viscosity-independent solvent effects. A clear discrimination between trapping and preassociation mechanisms has been found for general-acid catalysis of the addition to *p*-chlorobenzaldehyde of methoxyamine, which is inhibited by a factor of 12 in 50% glycerol, and of acetylhydrazide, which is independent of glycerol concentration.⁸ Water-glycerol mixtures have been used successfully to provide evidence for a diffusion-controlled step in the hydrolysis of 2-methyl- Δ^2 -thiazoline³¹ and *N*-*n*-propyldiisopropylmaleamic acid.³² Solvent effects are important for catalysis by ethylphosphonate dianion of the transimination of benzhydrylidenedimethylammonium ion and hydroxylamine through a diffusion-controlled trapping mechanism. The rate of this reaction is increased twofold in 45% glycerol but is increased eightfold in 45% methanol.³³

The secondary α -deuterium isotope effects for the reactions of formate esters determined by Kirsch, Cordes, and their co-workers provide further evidence for a transition from a trapping to a preassociation mechanism with decreasing basicity of nitrogen nucleophiles. The hydrazinolysis of methyl formate exhibits a secondary isotope effect of $k_D/k_H = 1.38$ that is consistent with formation of the tetrahedral addition intermediate T^\ddagger in a fast equilibrium step followed by rate-limiting proton transfer.³⁴ However, the general-acid-catalyzed reaction of the much less basic semicarbazide with 4-methoxyphenyl formate, a reaction that is very similar to the reaction described here, exhibits a value of $k_D/k_H = 1.14$ that supports a preassociation mechanism with rate-limiting amine attack and a transition state in which the N-C bond is only partially formed.¹⁰

There are now three classes of reaction in which a change from a trapping mechanism to a preassociation mechanism has been demonstrated as the nucleophilic reagent is made less basic, so that the initial addition intermediate reverts to reactants more rapidly: (1) the aminolysis of esters, (2) general-acid catalysis of the addition of thiol anions to acetaldehyde to give hemithioacetals,⁹ and (3) general-acid catalysis of the addition of nitrogen nucleophiles to benzaldehydes.^{7,8}

The Isotope Effect Maximum. Maxima in solvent deuterium isotope effects at $\Delta pK = 0$ have been observed for general-acid catalysis of the addition of methoxyamine to *p*-methoxybenzaldehyde³⁵ and for general-base catalysis of the transimination of hydroxylamine and benzhydrylidenedimethylammonium ion.³³ These maxima are much sharper than those for proton transfer to or from carbon. The Brønsted plots for both of these reactions follow the Eigen curves that are expected for a simple trapping mechanism^{33,35,36} and the decrease in the isotope effect on both sides of the maximum can be explained by a change in rate-limiting step to diffusional encounter or separation of the catalyst and addition intermediate, without invoking a change in the isotope effect for the proton-transfer step itself. The isotope effect maxima may be accounted for quantitatively by the classical three-step Eigen mechanism for proton transfer in which the proton-transfer step itself, with an isotope effect of $k_H/k_D = 3-5$, is partly rate limiting only in the region near $\Delta pK = 0$.^{33,37} This proton-transfer

(30) It is possible that the large rate constant of 10^{11} s^{-1} at $\Delta pK = 0$ is a consequence of smaller requirements for solvation changes in the proton transfer of a preassociation mechanism than in an ordinary proton transfer. In the preassociation mechanism the oxy anion base is suddenly generated with a hydrogen bond to HA , so that proton transfer can occur rapidly with a minimal requirement for solvent rearrangement around oxygen. Such rearrangement is likely to be more significant for a fully solvent-equilibrated oxy anion.

(31) Cerjan, C.; Barnett, R. E. *J. Phys. Chem.* **1972**, *76*, 1192-1195.

(32) Aldersley, M. F.; Kirby, A. J.; Lancaster, P. W.; McDonald, R. S.; Smith, R. S. *J. Chem. Soc., Perkin Trans. 2* **1974**, 1487-1495.

(33) Fischer, H.; DeCandis, F. X.; Ogdan, S. D.; Jencks, W. P. *J. Am. Chem. Soc.* **1980**, *102*, 1340-1347.

(34) Bilkadi, Z.; de Lorimer, R.; Kirsch, J. F. *J. Am. Chem. Soc.* **1975**, *97*, 4317-4322.

(35) Bergman, N.-Å.; Chiang, Y.; Kresge, A. J. *J. Am. Chem. Soc.* **1978**, *100*, 5954-5956.

(36) Rosenberg, S.; Silver, S. M.; Sayer, J. M.; Jencks, W. P. *J. Am. Chem. Soc.* **1974**, *96*, 7986-7998.

step could occur through a normal activation-limited process, tunneling, or proton movement coupled to solvent rearrangement.^{19,38-40} It is not possible to determine whether or not there is a change in the isotope effect for this step with changing ΔpK because of the limited range of ΔpK in which it is kinetically significant.

The preassociation mechanism provides a larger "window" in which the proton transfer step, k_p , is largely rate determining, because the diffusional encounter step is bypassed and the k_1' step does not become rate determining until the acid strength increases to pK_a 3-4 (Figure 4). The left-hand limb of the sharp maximum in the solvent isotope effect for general-acid catalysis of the methoxyaminolysis of phenyl acetate (Figure 5) occurs in the region in which the proton-transfer step is still rate determining for acids of pK_a 4-6, so that it is necessary to account for a decrease in the isotope effect of the proton transfer step, k_p (eq 6), with increasing acid strength.

The dashed line in Figure 5 shows that the change in rate-determining step to amine attack with hydrogen bonding to HA (k_1') does not account for the observed sharp decrease in the isotope effect for acids of $pK_a < 6$. This line was calculated by using the same parameters as for the Brønsted plot of Figure 4 and solvent deuterium isotope effects of 5 for k_p and 1.25 for k_{HA}^{dc} and k_b . Variation of these parameters does not improve the fit for acids of $pK_a < 6$. However, the decrease in the isotope effect for acids of $pK_a > 7$ can be accounted for by a change to diffusional separation of $T^+ \cdot A^-$ (k_b , eq 6) as the rate-limiting step for weak acids, by using a larger isotope effect. The problem, then, is to explain how proton transfer can be largely rate limiting for acids of pK_a 4-6 without giving a significant isotope effect; i.e., how can there be a significant barrier for proton transfer that is crossed at an almost equal rate by protium and deuterium?

We consider two mechanisms for changing isotope effects, either of which appears to provide a satisfactory explanation for the isotope effect maximum of Figure 5. First, the zero-point energy of the A-H bond may be retained in the symmetric stretching vibration of an early transition state for proton transfer in which this vibration involves motion of the proton orthogonal to the reaction coordinate, as described by Melander and Westheimer.^{41,42} In a reaction coordinate-energy diagram with separate axes for bonding to the proton donor and acceptor this corresponds to a nearly vertical or horizontal reaction coordinate that passes through the transition state in a direction almost parallel to one of the axes.⁴³ The very rapid change from a symmetric to an asymmetric structure of the transition state with changing acid strength that is required by this explanation is not unreasonable for a simple proton transfer between electronegative atoms, because of the very small barrier for such transfers. The rate of change in the structure of the transition state as the structure of the reactants is changed depends inversely on the sharpness of the curvature of the energy surface at the transition state^{44,45} and a

(37) Cox, M. M. Ph.D. Thesis, Brandeis University, 1979. The isotope effect curve for the former reaction was calculated from eq 2 and rate constants (for the reaction in water): $\log k_p = 10.7 + 0.5\Delta pK$, $\log k_{-p} = 10.7 - 0.5\Delta pK$, $\Delta pK = pK_{T^+} - pK_{HA}$, $k_b = k_{-a} = 10^{11} s^{-1}$, $k_{-b} = k_a = 10^{10} M^{-1} s^{-1}$, $K_1 = 1.78 \times 10^{-8} M^{-1}$; $k_p(H_2O)/k_p(D_2O)$ and $k_{-p}(H_2O)/k_{-p}(D_2O) = 4$ or 5. The rate constants for diffusion-controlled steps (k_a , k_{-a} , k_b , and k_{-b}) were assumed to be decreased by 20% in D_2O .

(38) (a) Bell, R. P.; Sachs, W. H.; Tranter, R. L. *Trans. Faraday Soc.* **1971**, *67*, 1995-2003. (b) Bell, R. P. "The Proton in Chemistry"; Cornell University Press: Ithaca, NY, 1973; p 250.

(39) Kurz, J. L.; Kurz, L. C. *J. Am. Chem. Soc.* **1972**, *94*, 4451-4461. See also: Ritchie, C. D.; Skinner, G. A.; Badding, V. G. *Ibid.* **1967**, *89*, 2063-2071. Kreevoy et al. have observed significant isotope effects for hydrogen-bonded protons of the kind that would be expected in the coupled mechanisms of Kurz and Kurz (Kreevoy, M. M.; Liang, T.-m.; Chang, K.-C. *J. Am. Chem. Soc.* **1977**, *99*, 5207-5209).

(40) German, E. D.; Kharkats, Y. I. *Izv. Akad. Nauk SSSR, Ser. Khim.* **1972**, *21*, 1031-1038 (*Bull. Acad. Sci. USSR, Div. Chem. Sci. (Engl. Transl.)* **1972**, *21*, 987-993). Brüniche-Olsen, N.; Ulstrup, J. *J. Chem. Soc., Faraday Trans. 1* **1979**, 205-226.

(41) Melander, L. "Isotope Effects on Reaction Rates"; Ronald Press: New York, 1960; pp 24-32.

(42) Westheimer, F. H. *Chem. Rev.* **1961**, *61*, 265-273.

(43) More O'Ferrall, R. A. In "Proton-Transfer Reactions"; Caldin, E. F., Gold, V., Eds.; Wiley: New York, 1975; Chapter 8.

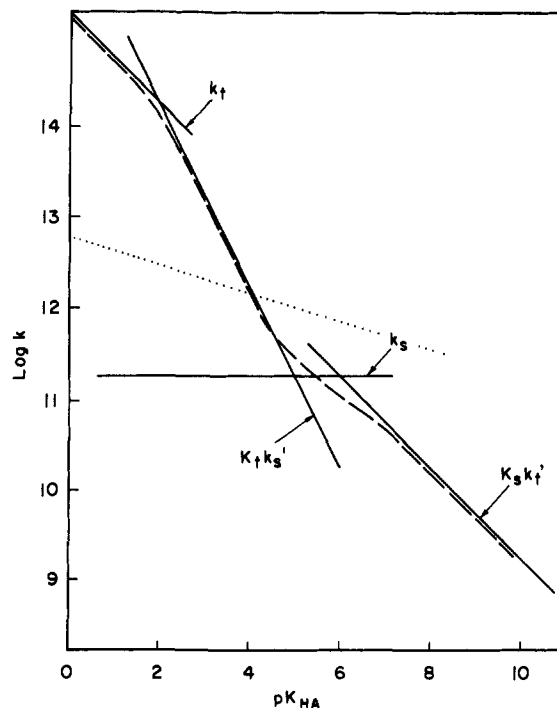
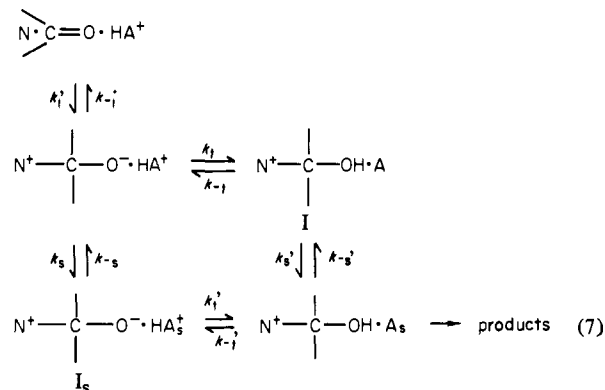


Figure 6. Schematic Brønsted curves to show how a mechanism for proton transfer involving kinetically significant solvation changes (eq 7 and 8) can cause changes in rate-limiting step and an isotope effect maximum. The dashed line is the resulting rate constant for the k_p step of eq 6, and the dotted line shows how the attack step, k_1' , becomes rate limiting for acids of $pK_a < 4$.

very low barrier might be expected to have a small negative curvature, because it is not well separated from the positive curvature of the well for the reactants. The transition state can then slide relatively easily over the energy surface as the energy of the proton donor is increased.

The second explanation is that there is still another change in rate-limiting step in the proton-transfer process as the acid becomes stronger, to a step that does not involve loss of zero-point energy. Following a suggestion of Kreevoy that the isotope effect maximum may represent a solvation effect,⁴⁶ we propose the mechanism of eq 7, in which the k_t terms describe proton transfer, the k_s terms



describe changes in solvation, and the subscript s refers to an arrangement of solvent that is optimal for the products rather than for the reactants. This model accounts for the data by providing two alternative pathways for the proton transfer.

The change in rate-limiting step can be explained as follows. With weak acids the lower path is followed, with solvent rear-

(44) Thornton, E. R. *J. Am. Chem. Soc.* **1967**, *89*, 2915-2927.

(45) Marcus, R. A. *J. Phys. Chem.* **1968**, *72*, 891-899.

(46) Kreevoy, M. M., personal communication. See also: Kreevoy, M. M.; Kretschmer, R. A. *J. Am. Chem. Soc.* **1964**, *86*, 2435-2440; Albery, W. J.; Campbell-Crawford, A. N.; Curran, J. S. *J. Chem. Soc., Perkin Trans. 2* **1972**, 2206-2217.

Table II. Rate Constants for the Proton Transfer Mechanism of Equation 7

constant	series A	series B
	k_x	
$\log k_t$	$12 + 0.5\Delta pK$	$12.5 + 0.5\Delta pK$
$\log k_{-t}$	$13.5 - 0.5\Delta pK$	$13 - 0.5\Delta pK$
$\log k_s'$	11.25	11.25
$\log k_{-s}'$	9.75	10.75
	k_y	
$\log k_t'$	$12 + 0.5\Delta pK$	$12.5 + 0.5\Delta pK$
$\log k_{-t}'$	$11 - 0.5\Delta pK$	$11.5 - 0.5\Delta pK$
$\log k_s$	11.25	11.25
$\log k_{-s}$	12.25	12.25
pK_{T^+}	6.5	5.5

rearrangement first and then proton transfer, whereas stronger acids follow the upper path with proton transfer prior to solvent rearrangement. The two intermediates I and I_s are of relatively high energy because of non-optimal solvation. The changes in rate-limiting step within each pathway and between the two pathways are illustrated in Figure 6. Proton transfer from a relatively weak acid will occur through the lower path via I_s with k_t' rate limiting because proton transfer through the upper path generates the unstable intermediate I, which immediately returns to reactants ($k_{-t} > k_t, k_s'$). As the acid becomes stronger the proton transfer via k_t' becomes faster and the pK-independent change in solvation k_s becomes rate limiting. This step could involve rearrangement of water molecules solvating RNH₃⁺, for example. For still stronger acids the reaction follows the upper path because the rate and equilibrium constants for the formation of I become so favorable that proton transfer occurs in spite of the unfavorable solvation of I. At first the solvation change k_s' is rate limiting because k_{-t} is still very fast. This step has a large sensitivity to acid strength because it is preceded by the proton-transfer step with the equilibrium constant $K_t = k_t/k_{-t}$. With the strongest acids k_{-t} becomes relatively slow and k_t becomes rate limiting. The changes in rate-limiting step occur because of the different dependencies of the rate constants for the two pathways on ΔpK —the rate and equilibrium constants for the proton-transfer step depend on ΔpK but the rate constants for the solvation steps, k_s and k_s' , are independent of ΔpK , in accord with Grunwald's finding that the rate of departure of a hydrogen-bonded water molecule from an amine has little or no dependence on pK.⁴⁷

Rate constants for the proton-transfer step, k_p in eq 6, were calculated from eq 8 in which k_x and k_y refer to the upper and

$$k_p = k_x + k_y = \frac{k_t k_s'}{k_{-t} + k_s'} + \frac{k_s k_t'}{k_{-s} + k_t'} \quad (8)$$

lower paths of eq 7, respectively, and from the rate and equilibrium constants in series A (Table II) by assuming deuterium isotope effects of $k_{HA}/k_{DA} = 12$ for the proton-transfer steps. These values of k_p give a good fit to the observed Brønsted plot, as shown by the dot-dashed line in Figure 4, and account for the sharp maximum in the isotope effect, as shown by the solid line in Figure 5; the contributions of the different steps are shown in Figure 6. The isotope effect decreases for acids of pK > 7 because the diffusion-controlled separation step, k_b , becomes rate limiting and decreases for acids of pK < 6 because the solvent reorganization steps, k_s and k_s' , become rate limiting.

We do not suggest that the absolute values of the rate constants for solvation changes and proton transfer in Table II are correct but only wish to point out that it is possible to choose values for these constants that are consistent with the observed rate constants and isotope effects and are not altogether unreasonable. An identical fit to the lines in Figures 4 and 5 is provided by the constants in series B of Table II, which are based on a lower pK for the addition intermediate. (It should be noted that we have

adopted the convention that all pK_a values refer to solvated species in free solution, with the consequences that $k_t \neq k_{-t}$ and $k_t' \neq k_{-t}'$ when $\Delta pK = 0$ and that some of the barriers for proton transfer in one direction become vanishingly small with increasing acid strength.⁴⁸ The k_t step never becomes rate limiting for this preassociation mechanism because the k_t' step is rate limiting at low pK_{HA}. It may also be noted that it is likely that the oxyanion of T[±] never reaches the equilibrium state of solvation that is expected for an oxyanion in water, because of its fleeting existence and its solvation by HA⁺.)

The mechanism of eq 7 may be made possible by the similar, small barriers for the proton transfer and solvent rearrangement steps, as well as the different dependencies of these steps upon ΔpK in this system. In contrast, electron-transfer reactions may proceed by a rapid jump of the electron between the two reactants when solvent rearrangement and other processes have occurred in such a way as to give equal free energies for the electron in the two positions.⁴⁹ The proton-transfer reaction differs in that the proton-transfer step, k_t or k_t' , has a significant barrier that must be passed over or tunneled through and gives rise to the observed deuterium isotope effect. The solvent rearrangement may also occur in discrete steps with rate constants such as the breaking of a hydrogen bond rather than occur through a continuum of states. It is likely that a complete description of the proton-transfer process would include a number of paths with differing amounts of solvation change before proton transfer in addition to the two limiting paths of eq 7. Kurz and Kurz have described several such paths, of which their second uncoupled mechanism is similar to eq 7 with k_s or k_s' rate limiting.³⁹ It is also probable that the dependencies on ΔpK of the actual proton transfer steps, k_t and k_t' , will become larger than 0.5 as ΔpK becomes large and unfavorable (and smaller than 0.5 as it becomes favorable). More information about fast proton-transfer processes is needed before these possibilities can be evaluated quantitatively, but it does not appear likely that such information will alter the general features of the model.

A model has been described for proton transfer by tunneling after excitation of low frequency intramolecular and solvent modes.⁴⁰ This model can give a maximum in the isotope effect for proton transfer from carbon acids as a consequence of varying amounts of deuterium transfer to or from an excited state with varying ΔpK . We have not attempted to apply this model to the isotope effect maximum described here.

Several other hypotheses fail to account for the isotope effect maximum with its sharp falloff for acids of pK_a < 6. A decrease in the contribution of tunneling as the proton transfer becomes more favorable might account for some decrease in the isotope effect.^{38,50} However, a decrease in the tunneling contribution cannot account for the small isotope effects that are observed on both sides of the maximum in this and other reactions. Some other mechanism such as a Melander–Westheimer effect must be invoked to explain how the proton can cross the barrier in the rate-limiting transition state with little or no loss of the zero-point energy difference between hydrogen and deuterium in the ground state, or there must be a change to a rate-limiting solvent reorganization or diffusion step so that the proton is not being transferred in the transition state. The primary deuterium isotope effect in the E2 elimination reaction of PhCH₂CH₂NMe₃⁺ has recently been separated into a contribution from tunneling, which is constant, and a semiclassical isotope effect, which accounts for the observed isotope effect maximum in Me₂SO–water mixtures.⁵¹

(48) The species T[±]·HA⁺ is expected to be stabilized by hydrogen bonding and electrostatic interactions, so that the true values of the rate and equilibrium constants for its reactions will be smaller than the values given in Table II. Since the amount of this stabilization is unknown, we have chosen to use rate and equilibrium constants based on pK_a values for the free reactants. This has no effect on the calculated rate constants or isotope effects, which depend only on rate constant ratios and the free energies of transition states relative to the free reactants. However, it does lower the pK value at which $\Delta pK = 0$ for species in eq 7 so that the observed isotope effect maximum occurs above this value, in the region in which k_t' is largely rate limiting.

(49) Marcus, R. A. *J. Chem. Phys.* **1956**, *24*, 966–978.

(50) Reference 38b, p 250.

(47) Grunwald, E.; Ralph, E. K., III *J. Am. Chem. Soc.* **1967**, *89*, 4405–4411.

The existence of an isotope effect maximum means that there is a sharper curvature of the Brønsted curve for protium than for deuterium acids near $\Delta pK = 0$. This can be described formally by the approach of Marcus, Kreevoy, Kresge, and others^{45,52,53} by assigning a smaller intrinsic barrier for the transfer of protium than of deuterium, and a satisfactory fit to the data of Figure 5 may be obtained by assigning a value of $\Delta G_0^\ddagger = 0.6 \text{ kcal mol}^{-1}$.² However, this formalism does not provide an explanation for the isotope effect maximum and may even be misleading.

According to the Marcus treatment there are two different reasons why the isotope effect can decrease with increasing ΔpK . First, at sufficiently large ΔpK the ordinary chemical barrier for reaction will disappear and the reaction will be limited by the work required to bring the reactants in position to react, w^\ddagger , and (in the unfavorable direction) by $\Delta G^{0'}$ for the reaction. The work term w^\ddagger is normally independent of ΔpK , and for proton transfer between electronegative atoms it corresponds to diffusion together of the reactants, steric effects, and possibly a rearrangement of

solvent. The latter two terms are small or insignificant for a large favorable ΔpK because the observed rate constants approach or reach the diffusion-controlled limit. This corresponds to a change in rate-limiting step with decreasing pK_a of the acid (k_a , eq 1, and dotted line, Figure 4), and does not account for the isotope effect maximum in this reaction, as described above. Second, an isotope effect maximum could be caused by different intrinsic barriers, $\lambda/4$ or ΔG_0^\ddagger , for protium and deuterium that give different curvatures of the Brønsted lines for the two isotopes. Different shapes or curvatures of the energy barriers can give rise to different rates of change of the barriers with changing reactant structure.^{44,45} However, it is usually assumed that the potential barriers for hydrogen and deuterium are identical and that isotope effects are caused primarily by differences in zero-point energy and tunneling frequencies. Furthermore, this description does not provide an explanation for the isotope effect maximum, so that it is still necessary to invoke the Melander–Westheimer effect or some other explanation to account for how the difference in the zero-point energies for hydrogen and deuterium in the reactants can be retained in the transition state when ΔpK becomes large and the isotope effect becomes small.

(51) Kaldor, S. B.; Saunders, W. H., Jr. *J. Am. Chem. Soc.* **1979**, *101*, 7594–7599.

(52) Kreevoy, M. M.; Oh, S.-w. *J. Am. Chem. Soc.* **1973**, *95*, 4805–4810. Kreevoy, M. M. In "Isotopes in Organic Chemistry"; Buncl, E., Lee, C. C., Eds.; Elsevier: New York, 1976; Vol. 2, pp 1–31.

(53) Kresge, A. J.; Sagatys, D. S.; Chen, H. L. *J. Am. Chem. Soc.* **1977**, *99*, 7228–7233.

Supplementary Material Available: A table and three figures describing experimental rate constants (9 pages). Ordering information is given on any current masthead page.

Concerted Bifunctional Proton Transfer and General-Base Catalysis in the Methoxyaminolysis of Phenyl Acetate¹

Michael M. Cox and William P. Jencks*

Contribution No. 1341 from the Graduate Department of Biochemistry, Brandeis University, Waltham, Massachusetts 02254. Received July 7, 1980

Abstract: The bifunctional acid–base catalysts cacodylic acid, bicarbonate, and the monoanions of phosphate, substituted phosphonates, and methylarsonate are up to 10^2 – 10^3 more effective than monofunctional acids or bases of comparable pK for catalysis of the methoxyaminolysis of phenyl acetate. The absence of the downward break in the Brønsted plot and the solvent isotope effect maximum that are observed with monofunctional acid catalysts when proton transfer becomes partially rate limiting indicates that these bifunctional catalysts avoid this stepwise proton-transfer step. It is concluded that the two proton transfers occur through a mechanism with no detectable barrier or isotope effect, which appears to be concerted and is so fast that proton transfer never becomes kinetically significant; the rate-limiting step is amine attack with hydrogen bonding by the catalyst. Glycine and water show smaller rate increases that probably represent stepwise bifunctional proton transfer through a nine-membered ring or two water molecules in a one-encounter mechanism. Pyrazole and triazole show little or no enhancement of catalytic activity, indicating that bifunctional proton transfer through a seven-membered ring is relatively unfavorable in aqueous solution. Catalysis by monofunctional bases follows a nonlinear Brønsted plot and is attributed to a preassociation mechanism analogous to that for general-acid catalysis.

"Concerted acid–base catalysis" means different things to different people including (1) a reaction in which several processes occur in one step with no intermediate, (2) proton transfer that is electronically coupled to some other bond-making or -breaking process, (3) a term in a rate law that contains both an acid and a base molecule, and (4) bifunctional catalysis by a single molecule containing both an acidic and a basic group. We will be concerned here with *bifunctional acid–base catalysis* by a single molecule and the extent to which this catalysis is *concerted* in the sense of two processes occurring with no intermediate step. Bifunctional acid–base catalysis is a venerable and popular hypothesis to help

explain the chemical mechanism of enzymic catalysis and has been studied extensively in nonenzymic reactions following the pioneering work of Lowry and Swain and Brown.^{2,3} The rate increases from such catalysis in aqueous solution are generally not dramatic because water is itself a good acid–base catalyst, possibly a bifunctional acid–base catalyst. It has been suggested that fully concerted bifunctional catalysis that involves changes in bonding to heavy atoms is rare or nonexistent because of the low probability that all of the requirements for the several processes that must take place at once can be met in a single, low-energy transition state.⁴

(1) Supported by grants from the National Science Foundation (Grant BG-31740) and the National Institutes of Health (Grants GM20888 and GM20168). M.M.C. was supported by a training grant from the National Institutes of Health (Grant 5-T01-GM00212).

(2) Lowry, T. M.; Falkner, I. J. *J. Chem. Soc.* **1925**, *127*, 2883–2887. Lowry, T. M. *Ibid.* **1927**, 2554–2565;

(3) Swain, C. G.; Brown, J. F., Jr. *J. Am. Chem. Soc.* **1952**, *74*, 2534–2537, 2538–2543.